Journal of Materials Chemistry A

ROYAL SOCIETY OF CHEMISTRY

PAPER

View Article Online
View Journal

Cite this: DOI: 10.1039/d6ta00654j

Photocatalytic semi-hydrogenation of acetylene to ethylene in water powered by a copper-functionalized hydrogen-bonded organic framework

Brando Adranno, † Anna Fortunato, † Sharon Silloni, Marianna Barbieri, Stefano Agnoli, Luka Đorđević * and Francesca Arcudi *

Received 23rd January 2026
Accepted 9th April 2026

DOI: 10.1039/d6ta00654j

rsc.li/materials-a

Light-driven approaches for the selective semi-hydrogenation of acetylene to ethylene are emerging as sustainable alternatives to conventional thermochemical purification methods. The realization of a highly selective, robust, and recyclable photocatalyst that avoids noble metals, operates under visible light, and uses water as the proton source remains a major challenge. Here, we report the first demonstration of a supramolecular crystalline material as photocatalyst for the visible-light powered conversion of acetylene to ethylene. The catalyst is a copper-loaded hydrogen-bonded organic framework 1,3,6,8-tetrakis(*p*-benzoic acid)pyrene (Cu@HOF), which integrates light-harvesting and catalytic function within a single material and uses water as the proton source. Under a pure acetylene atmosphere, Cu@HOF achieves an overall ethylene production of 3.01 mol g^{-1} Cu with ≥99.9% selectivity after 16 h of irradiation. Under the industrially relevant conditions of a mixed acetylene/ethylene atmosphere, Cu@HOF enables near 100% acetylene conversion within only 75 min. The heterogeneous nature of the catalyst allows straightforward recovery and reusability, retaining catalytic activity under industrial mixture conditions over at least four consecutive cycles.

Department of Chemical Sciences, Università di Padova, Via Marzolo 1, Padova, Italy. E-mail: luka.dordevic@unipd.it; francesca.arcudi@unipd.it

† These authors contributed equally to this work.

Francesca Arcudi

Francesca Arcudi received her PhD from the University of Trieste in 2017 and was a post-doctoral fellow at Northwestern University from 2018 to 2022. In 2023, she began her independent career at the University of Padova through the Rita Levi-Montalcini Programme and she is now Associate Professor. Her research focuses on developing new strategies for light-driven chemical transformations aimed at the sustainable production of fuels and commodity chemicals. In 2025, she was awarded a FIS grant (Italian Science Fund) to support her research team's work on photocatalytic systems based on inorganic complexes and functional materials for solar energy conversion and chemical synthesis.

Introduction

Ethylene (C_2H_4) is one of the most valuable commodity chemicals underpinning the production of polyethylene and a wide range of other plastics. It is mainly produced *via* steam cracking of hydrocarbon feedstocks,[1,2] a process that inevitably generates small amounts of acetylene as a by-product.[3] Even trace levels of acetylene act as poisons for Ziegler–Natta polymerization catalysts,[4] making acetylene removal a critical purification step at the very beginning of the supply chain. Industrial purification of crude ethylene is traditionally achieved *via* thermocatalytic hydrogenation of acetylene. This process is economically and energetically demanding, as it requires high temperatures and pressures, the use of Pd-based catalysts, and a continuous co-feed of H_2 gas.[3,4] Moreover, over-hydrogenation to ethane, which is itself detrimental to polyethylene production, commonly occurs, limiting the overall selectivity of the acetylene to ethylene conversion.[3–5]

To address these challenges, an ideal acetylene purification strategy should simultaneously (i) replace noble metals with earth-abundant transition metals, (ii) avoid the use of molecular H_2 by relying on alternative and safer hydrogen sources, with water representing the most attractive option, and (iii) exploit electrochemical and, ideally, photocatalytic processes that enable acetylene semi-hydrogenation under mild

conditions using electrical or solar energy as the driving force, with photocatalysis being particularly attractive because it uses abundant photon energy. In this context, especially over the past three years, our groups and others have established homogeneous and heterogeneous photocatalytic systems that fulfil the design criteria outlined above, yet they remain largely confined only to cobalt-based photoredox catalysis with noble metals as photosensitizers.[6–19] Building on these advances, heterogeneous photocatalysts offer additional advantages in terms of stability, recyclability, and potential for practical and industrial implementation. To date, most heterogeneous photocatalytic systems developed for acetylene semi-hydrogenation rely exclusively on cobalt active sites that are embedded within metal–organic frameworks (MOFs)[7,8,10,18] and covalent organic frameworks (COFs).[14] While these materials benefit from structural definition and modularity, they often operate in tandem with an external noble metal-based photosensitizer, such as $Ru(bpy)_3^{2+}$, and typically require organic solvents, including acetonitrile or dimethylformamide, to achieve optimal performance.

Framework materials are attractive for photocatalytic applications due to their well-defined and synthetically tailorable architectures, which facilitate the establishment of structure–performance relationships.[20,21] While these features are also shared by hydrogen-bonded organic frameworks (HOFs),[22] which have recently emerged as promising platforms for photocatalysis owing to a number of distinctive advantages (see below), HOFs are yet to be explored in photocatalytic conversion of acetylene to ethylene to purify ethylene streams. Compared to other framework-based materials, HOFs can be synthesized using more straightforward preparation protocols and under milder conditions, and owe their structural stability to the combination of H-bonding and π–π stacking interactions. Their modular and flexible architectures enable the combination of light absorption efficiency, electron delivery efficiency and catalytic efficiency of active sites within a single material.[23–26] Important figures of merit for their use in photochemistry include their facile modification, which is particularly advantageous given that HOFs usually lack catalytic metal centers in their pristine skeletons, while their flexible structural tailorability provides great opportunity to anchor catalytic sites. Post-synthetic modification by immobilization of metal ions within the HOF skeleton through coordination interactions is indeed a simple yet effective method to introduce metal sites. In addition, hydrogen-bonding interactions are relatively weaker than coordination and covalent bonds found in MOFs and COFs, allowing reversible bond formation and dissociation between monomers, which can improve recyclability. Furthermore, the choice of monomeric precursors is crucial in determining not only the porosity but also the chemical properties, enabling the rational design of tailor-made HOFs. For example, incorporation of conjugated aromatic molecular units can impart strong light-harvesting capability.[27–29] A prominent example is the hydrogen-bonded organic framework 1,3,6,8-tetrakis(*p*-benzoic acid)pyrene (HOF-H_4TBAPy), a pyrene-based HOF that has recently demonstrated strong light-harvesting ability for UV and visible light and photocatalytic efficiency for the H_2 evolution reaction when incorporating both noble and non-noble metal sites.[30–38]

Here, we sought to explore a HOF-based photocatalyst for the light-driven semi-hydrogenation of acetylene to ethylene, targeting three main features that would advance the state of the art in framework-based catalysts for this important chemical reaction. Specifically, our design aims to deliver (i) an all-in-one photocatalytic system that integrates light absorption and catalysis within a single material, (ii) operation in water as both solvent and proton source, and (iii) stabilization of earth-abundant 3d transition metals beyond cobalt as catalytically active sites. The latter point is particularly relevant as it enables expansion of the palette of transition metals available for this reaction, which is important in light of increasing concerns associated with cobalt supply,[39] and is further motivated by the documented ability of other 3d transition metals, including Mn, Fe, Ni, and Cu, to mediate alkyne reduction reactions.[40] Cu-based materials have emerged as excellent catalysts for the selective and efficient electrocatalytic conversion of acetylene to ethylene, a behavior often attributed to the favorable balance between acetylene adsorption and ethylene desorption on copper catalytic sites.[41–45] In addition, HOFs are characterized by a porous structure that enables high surface active area while also exhibiting high water stability, ideally allowing water as both solvent and proton source for catalytic transfer hydrogenation. Building on this knowledge and recent efforts from our groups,[6–8,10,11,14,18,46] we envisioned an integrated heterogeneous system based on copper-functionalized HOF-H_4TBAPy (Cu@HOF) for the reduction of acetylene to ethylene *via* photocatalytic water-donating transfer hydrogenation, efficiently integrating the photocatalytic water splitting capability demonstrated for HOF-H_4TBAPy[30–38] with the electrocatalytic alkyne (including acetylene) hydrogenation activity of copper catalysts[41,42,45,47–59] (Fig. 1).

In this work, we report ethylene production powered by visible light at room temperature using water as the proton source. We demonstrate acetylene conversion to ethylene with ≥99.9% selectivity and an overall production of 3.01 mol g^{-1} Cu under a pure acetylene feed. The Cu@HOF photocatalyst is also highly competent under the industrially relevant conditions for ethylene purification, *i.e.* in the presence of excess ethylene, achieving near 100% conversion of acetylene to ethylene within just 75 minutes and with 99.8% selectivity. Importantly, the photocatalyst demonstrates reusability under industrial mixture conditions, retaining catalytic activity over at least four consecutive cycles. Finally, our study proposes a catalytic route in which the Cu(I) active species are protonated to form Cu–H intermediates, and the protons added to make the ethylene product originate from water.

Results and discussion

The preparation of the hydrogen-bonded organic framework and its subsequent Cu(II) incorporation were carried out using previously published procedures (for details see the SI).[32,33] We prepared bulk microcrystalline HOF-H_4TBAPy, in which H_4TBAPy assembles into a hydrogen-bonded organic

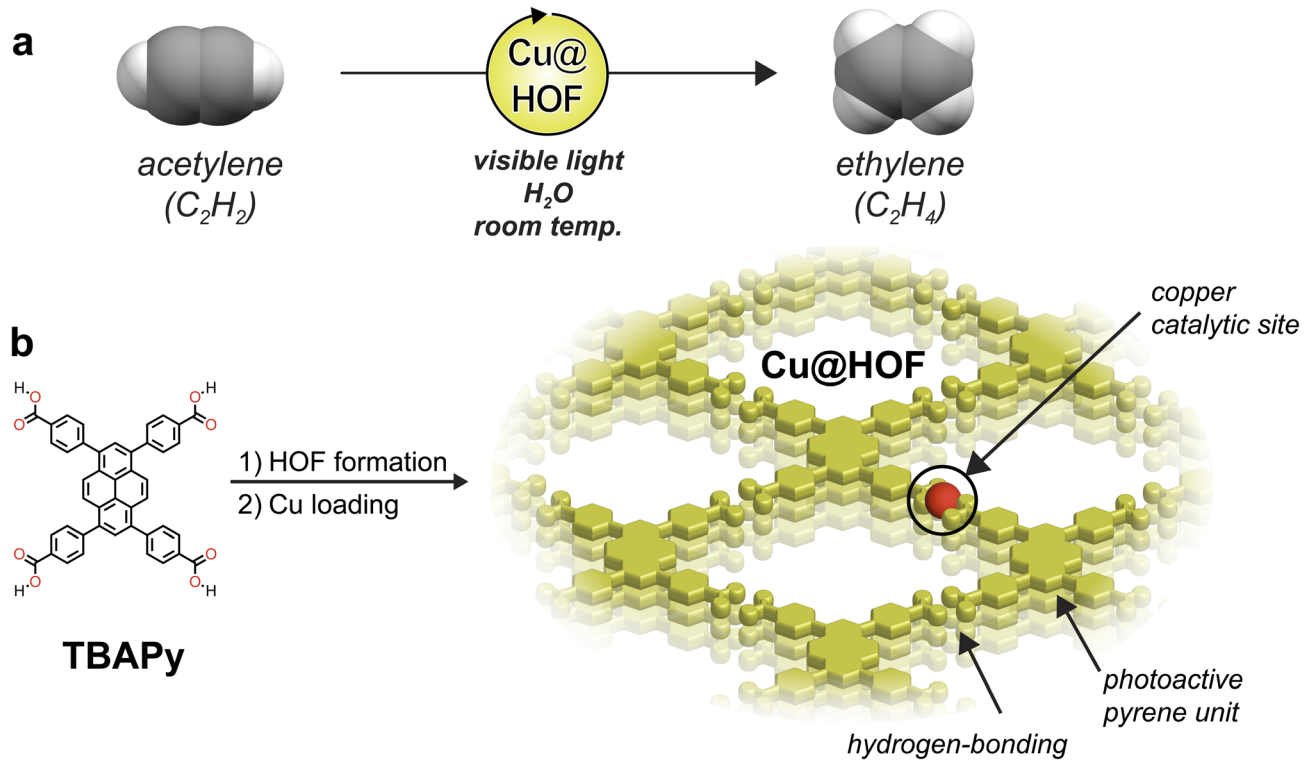

Fig. 1 (a) This work uses an all-in-one photocatalyst of Cu active sites anchored to a hydrogen-bonded organic framework (Cu@HOF) and water as the proton source at room temperature for the ≥99.9% selective semi-hydrogenation of acetylene to ethylene. (b) The Cu@HOF laid out in this study is obtained by post-synthetic functionalization of a hydrogen-bonded organic framework 1,3,6,8-tetrakis(*p*-benzoic acid)pyrene (HOF-H_4TBAPy) with Cu active sites.

framework *via* antisolvent-induced crystallization, followed by solvent-exchange and activation to open the one-dimensional micropore channels through soaking in acetone. Precipitation of H_4TBAPy under these solvent conditions provides better control over morphology and dispersion in aqueous media than the crystallization-solvent method,[30] ultimately yielding more catalytically active materials with a reported Brunauer–Emmett–Teller surface area of ~1530 $m^2\ g^{-1}$.[32,33] Activated HOF-H_4TBAPy was suspended in methanol and treated with an aqueous $Cu(NO_3)_2$ solution, followed by filtration and washing to afford Cu@HOF. The pores of the material were activated by drying the Cu@HOF powder in oven. The powder X-ray diffraction (PXRD) pattern of HOF-H_4TBAPy shows characteristic diffraction peaks at $2\theta = 4.4°$ and 6.2°, which are consistent with the typical eclipsed (*i.e.* AA) stacking mode (Fig. 2a) and in agreement with literature.[32,60,61] Broader diffraction features in the $2\theta = 23–28°$ range are attributed to π–π interaction between the H_4TBAPy units.[32] The Fourier transformed infrared (FTIR) spectrum of the HOF shows peaks between 3371 to 2478 cm^{-1}, which are attributed to the vibrational stretching of the –COOH groups connected *via* hydrogen bonding (Fig. S1),[33] further confirming the formation of the supramolecular structure. Transmission electron microscopy (TEM) of HOF-H_4TBAPy (Fig. 2b–d) reveals a fringe distribution of 2.02 nm, in good agreement with literature.[32] Both TEM (Fig. 2e and f) and PXRD (Fig. 2a) analyses of Cu@HOF show no significant differences compared to that of the metal-free HOF, indicating preservation of the framework and its crystalline lattice after copper incorporation and pointing to an ideally atomic dispersion of Cu atoms. The homogeneous distribution of Cu throughout the framework was further confirmed by energy-dispersive X-ray spectroscopy (EDXS, Fig. 2g). We quantified the amount of incorporated copper as 0.45% w/w by inductively coupled plasma (ICP-MS) analysis (Table S1). X-ray photoelectron spectroscopy (XPS) analysis identifies copper predominantly as Cu^{2+} species, as evidenced by the characteristic $2p_{3/2}$ peak at 933.6 eV, together with the presence of weak final state satellites features in the range 940–950 eV and 958–965 eV, respectively (Fig. S2).[62] The optical properties of HOF and Cu@HOF were investigated using diffuse reflectance UV-vis ((DR)UV-vis) spectroscopy (Fig. S3a). The corresponding Tauc plots yield optical bandgaps of 2.55 eV for Cu@HOF and 2.59 eV for HOF (Fig. S3b). Electrochemical measurements place the first reduction event of Cu@HOF at −1.15 V *vs.* Fc^+/Fc (Fig. S4).

We then investigated the photocatalytic activity of Cu@HOF for the semi-hydrogenation of acetylene using ascorbic acid (HAsc) as a sacrificial donor in ultrapure water. The reaction mixture was first placed under 1 atm of C_2H_2 and then illuminated with a 450 nm light-emitting diode (LED, 140 mW cm^{-2}). Details of purging and photocatalytic setups are published elsewhere.[6] The composition of the headspace after irradiation was assessed by a gas chromatograph equipped with both

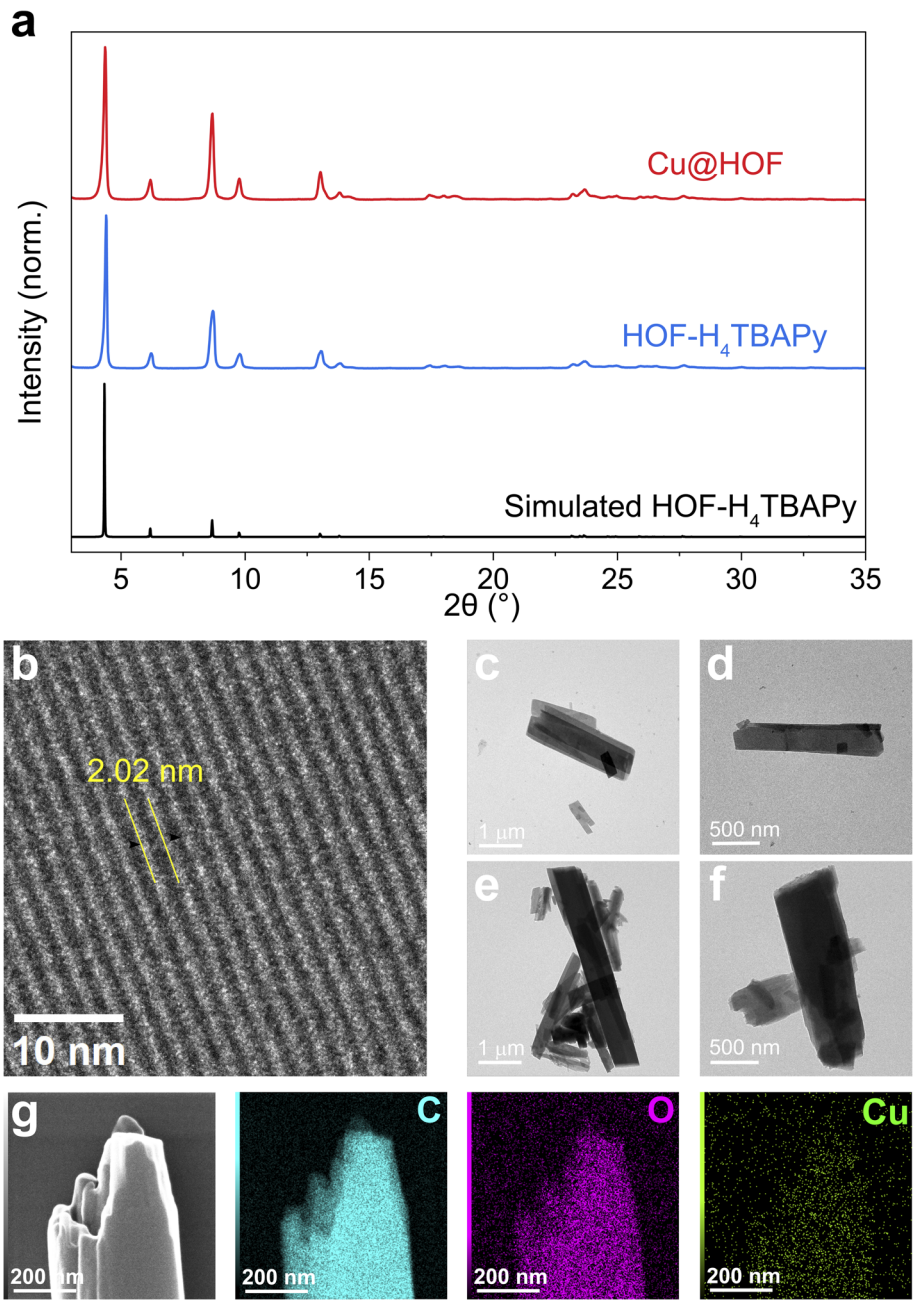

Fig. 2 (a) PXRD patterns of Cu@HOF (red), HOF-H_4TBAPy (blue), and simulated pattern of HOF-H_4TBAPy (black, from CCDC: 1826763).[63] (b) TEM image of 1D micropore channel structures of HOF-H_4TBAPy. (c) and (d) TEM images of HOF-H_4TBAPy. (e) and (f) TEM images of Cu@HOF. (g) EDXS mapping of Cu@HOF elements.

a thermal conductivity detector (TCD) and a flame ionization detector (FID), more details are provided in the SI. A typical gas chromatogram of the reaction mixture after irradiation shows conversion of acetylene to ethylene with no appreciable over-hydrogenation to ethane (Fig. S5 and S6).

Under optimized conditions, a catalytic mixture containing 1.0 mg of Cu@HOF and 0.1 M of HAsc at pH = 4.0 produced 2.86 ± 0.26 mol g^{-1} Cu of C_2H_4 after 4 h of irradiation, with ≥99.9% selectivity over C_2H_6. A minor amount of H_2 was detected (0.33 ± 0.02 mol g^{-1} Cu). Control experiments performed in the absence of light, sacrificial donor, catalyst, or C_2H_2 feedstock showed no detectable acetylene conversion (Fig. 3a), confirming the photocatalytic nature of the process. In addition, negligible C_2H_4 formation was observed when using the metal-free H_4TBAPy-HOF, indicating that the organic framework alone is insufficient to drive acetylene reduction and further highlighting the essential role of the Cu sites. Overall, these results demonstrate the first example of an all-in-one Cu-based photocatalyst for highly selective acetylene semi-hydrogenation.

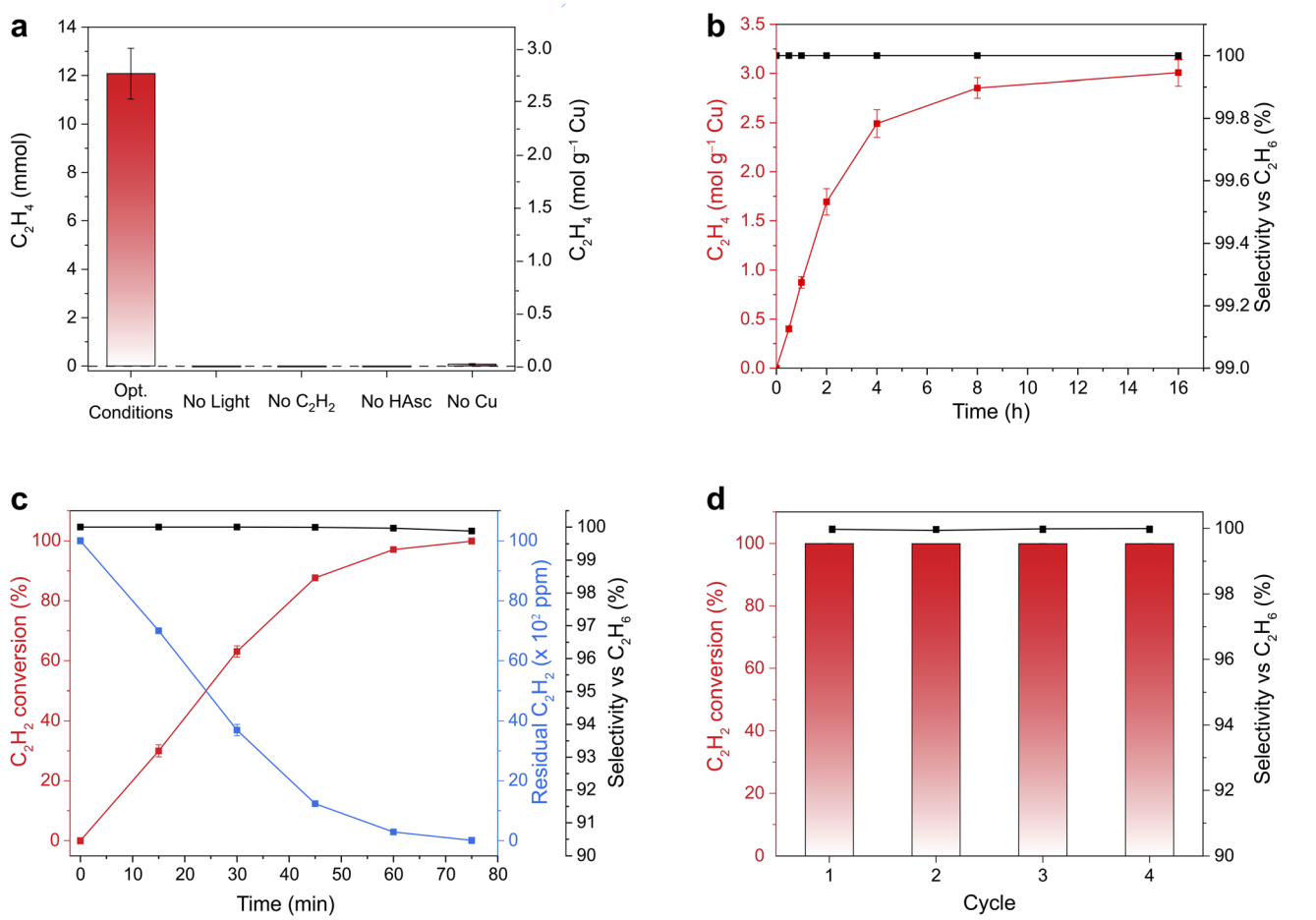

Fig. 3 (a) Total C_2H_4 production for the optimized reaction mixture containing 1.00 ± 0.05 mg Cu@HOF, 0.1 M of HAsc in 2.0 mL H_2O irradiated (450 nm, 140 mW cm^{-2}) for 4 h at pH = 4.0 ± 0.1 under C_2H_2 (≥99.5 vol%), and for reaction mixtures that differ from the optimized conditions as indicated by the axis labels. (b) Total ethylene production (red) and selectivity (black) as a function of irradiation time (450 nm, 140 mW cm^{-2}) for the system containing 1.00 ± 0.05 mg of Cu@HOF and 2.0 mL of 0.1 M aqueous solution of HAsc at pH = 4.0 ± 0.1 under C_2H_2 (≥99.5 vol%). (c) Plot of C_2H_2 conversion (%, red), residual C_2H_2 (ppm, blue), and C_2H_4 selectivity *vs.* C_2H_6 (%, black) as a function of irradiation time under industrially relevant conditions (1 vol% C_2H_2, 30 vol% C_2H_4, N_2 balance) for the photocatalytic system containing 3.50 ± 0.05 mg of Cu@HOF and 2.0 mL of 0.25 M aqueous solution of HAsc at pH = 4.0 ± 0.1. (d) Recyclability tests under industrial mixture conditions for the system containing 3.50 ± 0.05 mg of Cu@HOF and 2.0 mL of 0.25 M aqueous solution of HAsc at pH = 4.0 ± 0.1. Error bars represent the standard deviations for at least three separated experiments; uncertainty is ≤10%.

The optimized conditions for the photocatalytic semi-hydrogenation of acetylene were established through a series of screening experiments assessing the influence of pH, sacrificial donor concentration, and catalyst loading on ethylene production. The formation of our catalytic HOF-based material relies on hydrogen bonding between carboxylic acid groups, which have a reported pK_a of 6.9;[64] the structural stability of the framework was therefore evaluated under acidic conditions (pH < 6.0), as operation at higher pH values would compromise the crystalline structure. The semi-hydrogenation of C_2H_2 to C_2H_4 was examined across a range of pH values, revealing the activity trend pH 4.0 > pH 5.0 > pH 3.0 (Fig. S7), which reflects the combined influence of proton availability, the pH-dependent speciation, and reducing ability of ascorbic acid as sacrificial donor. At pH 4.0, evaluating the influence of HAsc concentration on the semi-hydrogenation of acetylene showed that increasing the HAsc concentration led to enhanced C_2H_4 production up to a concentration of 0.25 M (Fig. S8). Finally, variation of the catalyst amount showed that increasing the Cu@HOF amount resulted in a gradual decrease in ethylene production, with the highest activity obtained using 1.0 mg of Cu@HOF (Fig. S9).

The kinetic of ethylene production by the Cu@HOF-based photocatalytic system is shown in Fig. 3b. Illumination for 16 h of the photocatalytic mixture containing Cu@HOF produced 3.01 mol g^{-1} Cu of ethylene, representing a 2–100-fold improvement over previously reported framework-based catalysts that work in tandem with $Ru(bpy)_3^{2+}$, whereas Cu@HOF operates as an all-in-one system.[7,8,10,14,18] We detected no ethane, such that the selectivity for ethylene remains ≥99.9% (Fig. 3b).

We investigated the saturation in ethylene production after 16 h of irradiation. Re-addition experiments were carried out by first irradiating the sample for 16 h and then selectively re-adding the initial amount of either HAsc or Cu@HOF,

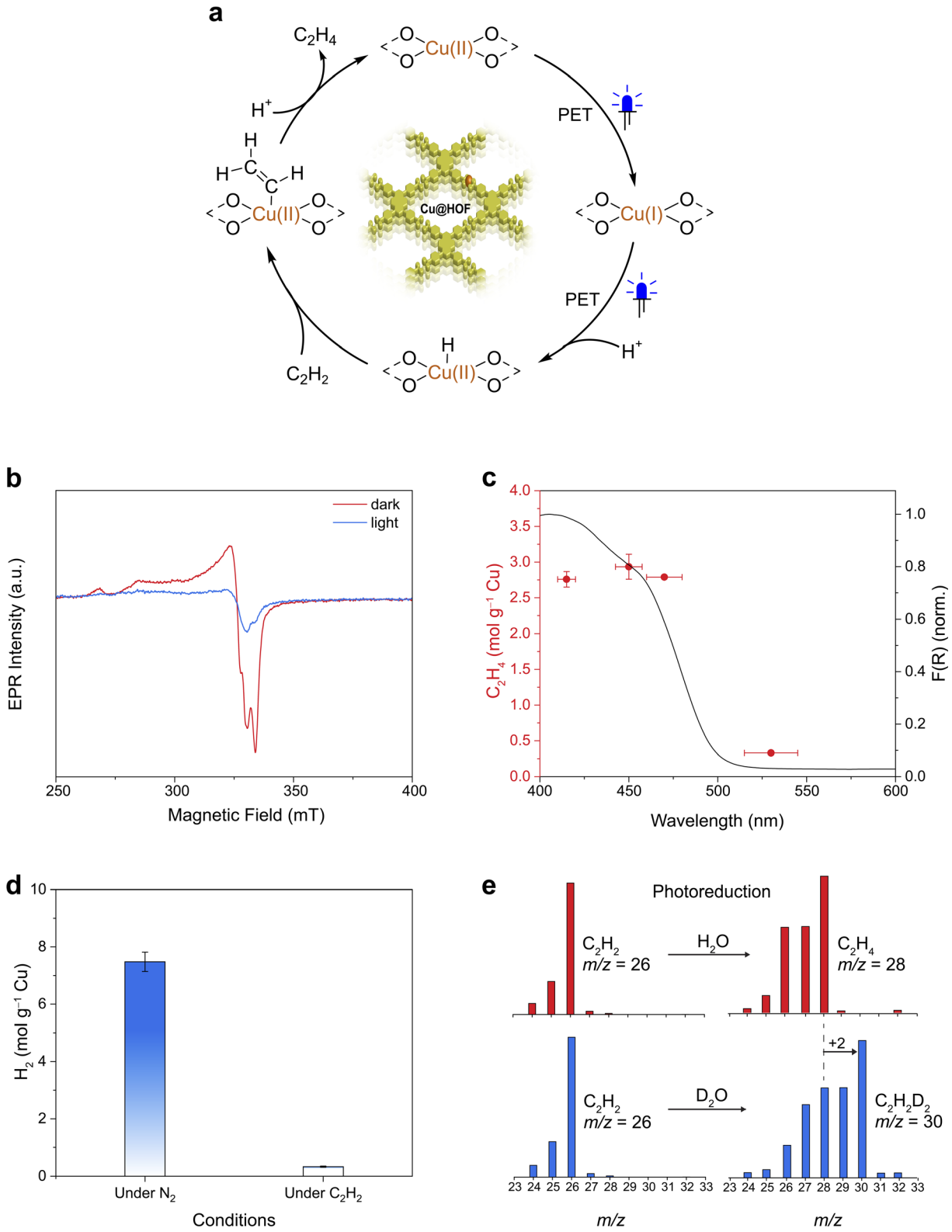

Fig. 4 (a) Proposed mechanism for the photoreduction of acetylene to ethylene by the Cu species anchored to the HOF *via* coordination interaction. (b) EPR spectra of Cu@HOF powder before (red) and after (blue) irradiation at 450 nm recorded at 77 K. (c) Ethylene production by the Cu@HOF optimized system (mol g^{-1} Cu, left axis, red dots) containing 1.00 ± 0.05 mg Cu@HOF in 2.0 mL of 0.1 M aqueous solution of HAsc at pH = 4.0 ± 0.1 under C_2H_2 and irradiated for 4 h as a function of irradiation wavelength (415, 450, 470, and 530 nm; 140 mW cm^{-2}) overlaid on the absorption spectrum of Cu@HOF (right axis, black line). (d) Photocatalytic H_2 evolution by the Cu@HOF-based system under N_2 *vs.* C_2H_2. (e) MS of acetylene feedstock (left) and of ethylene product (right) for the irradiated (450 nm) Cu@HOF system under C_2H_2 in MilliQ H_2O (red) or in D_2O (blue). The shift $m/z + 2$ in H_2O corresponds to incorporation of two hydrogens to produce C_2H_4 when starting with C_2H_2. The shift $m/z + 4$ in D_2O corresponds to incorporation of two deuterium to produce $C_2H_2D_2$ when starting with C_2H_2.

followed by further illumination. These experiments show that it is possible to restart catalysis only upon addition of Cu@HOF (Fig. S10), suggesting that cessation of catalysis is primarily due to catalyst deactivation. Following catalysis, both the PXRD pattern and the TEM images of Cu@HOF indicate a loss of crystallinity in the framework (Fig. S11 and S12), while elemental analysis by ICP-MS detects Cu leaching from the catalyst (Table S1), and XPS and electron paramagnetic resonance (EPR) analyses reveal partial reduction of the copper to the Cu(0) species (Fig. S13). We stress, however, that catalysis originates from Cu@HOF rather than from Cu species leached into solution. This conclusion is corroborated by "hot filtration" experiments, in which the full reaction mixture was irradiated for 4 h, the HOF was then removed by centrifugation and syringe filtration, and the supernatant was subsequently irradiated. Under these conditions, we observe no additional conversion of C_2H_2 to C_2H_4, which confirms that catalysis proceeds exclusively at Cu sites embedded within the HOF framework (Fig. S14).

Critically for potential industrial application, Cu@HOF selectively reduces acetylene to ethylene even in the presence of excess ethylene (1 vol% C_2H_2, 30 vol% C_2H_4, N_2 balance). This C_2H_4/C_2H_2 mixture represents a typical industrial ethylene feed and requires a catalyst that is not only highly active but also highly selective to suppress over-hydrogenation to ethane. Under these competitive conditions, Cu@HOF reduces the acetylene concentration from 10 000 ppm to undetectable levels while maintaining 99.8% selectivity toward ethylene over ethane (Fig. 3c). Notably, complete acetylene removal is achieved within 75 min, corresponding to a 3–77-fold improvement over previously reported $Ru(bpy)_3^{2+}$-sensitized framework catalysts (Table S2).[7,8,10,14,18] Importantly, the possibility that the framework promotes the C_2H_2 removal through adsorption rather than photocatalytic semi-hydrogenation was ruled out. This conclusion is supported by the unchanged C_2H_2 content measured in the presence of both Cu@HOF and HOF-H_4TBAPy framework, either before irradiation or after being kept in the dark for 75 min (Fig. S15). The heterogeneous nature of Cu@HOF enables straightforward recovery of the photocatalyst by centrifugation. Upon replenishment of the HAsc solution (0.25 M) and C_2H_4/C_2H_2 gas feed, the catalyst can be reused over four consecutive cycles while maintaining complete conversion of acetylene to ethylene in the headspace (Fig. 3d).

We propose a mechanism for the photocatalytic semi-hydrogenation of C_2H_2 by Cu@HOF (Fig. 4a) based on experimental observations and on mechanistic models reported for Cu-mediated systems and transition-metal-catalyzed acetylene reduction reactions.[49,50,59,65,66] EPR analysis of the Cu@HOF powder confirms the presence of isolated Cu(II) species with $g_{\parallel} = 2.32$ and $g_{\perp} = 2.04$ (Fig. 4b), consistent with previous reports that attribute these values to coordination by carboxylic acid groups.[33,37] Upon visible-light irradiation, the EPR signal intensity decreased significantly (Fig. 4b), indicating efficient photoreduction of Cu(II) to EPR-silent Cu(I) species *via* transfer of photogenerated electrons. This conclusion is further corroborated by wavelength-dependent photocatalytic experiments (Fig. 4c). Ethylene production closely follows the absorption profile of Cu@HOF, confirming that the framework operates as a genuine all-in-one photocatalyst, acting simultaneously as light absorber and catalytic platform within the visible region. As the excitation wavelength is progressively shifted toward longer wavelengths, the ethylene production decreases, mirroring the reduced optical absorption of the HOF scaffold. Together with the EPR results, these data demonstrate that visible-light excitation of Cu@HOF generates electron–hole pairs within the framework, and that the photogenerated electrons are responsible for reducing Cu(II) to catalytically active Cu(I) species.

The Cu@HOF photocatalyst evolves only a small amount of H_2 during acetylene semi-hydrogenation, and H_2 evolution is substantially suppressed when the reaction is conducted under a C_2H_2 atmosphere compared to an Ar atmosphere (Fig. 4d). This behavior indicates that H_2 evolution and acetylene reduction proceed through a common intermediate and that, under competitive conditions, acetylene reduction outcompetes proton reduction. It is well established that electro- and photocatalytic hydrogen evolution mediated by Cu complexes proceed through the formation of Cu–hydride species generated upon reduction of Cu(II) in the presence of a proton donor,[59,67,68] and that Cu–hydride intermediates can also participate in alkyne semi-hydrogenation reactions.[40,49,50] On this basis, we suggest that acetylene reduction in the Cu@HOF system proceeds through a Cu–H intermediate.

A major advantage of the Cu@HOF system with respect to sustainability is that it does not require an external feed of H_2, prompting investigation of the origin of the hydrogen atoms incorporated into the ethylene product. To further identify the proton source, isotope-labelling experiments were performed (Fig. 4e). When the reaction was carried out in H_2O using C_2H_2 as feedstock, gas chromatography-mass spectrometry analysis identified C_2H_4 as the reaction product. In contrast, the reaction of C_2H_4 in D_2O leads to the $C_2H_2D_2$ product. These experiments demonstrate unambiguously that acetylene is the precursor to the observed ethylene and that the protons incorporated into the C_2H_4 product originate from the aqueous solvent, confirming that water acts as the proton source in the Cu@HOF photocatalytic cycle.

Following Cu–H formation, acetylene activation is proposed to occur *via* hydrogen atom transfer (HAT), leading to the formation of a vinyl–Cu intermediate. This mechanistic assignment is supported by catalytic experiments performed in the presence of the radical scavenger TEMPO, which result in a marked suppression of ethylene formation (Fig. S16), indicating the possible involvement of radical intermediates in HAT pathways. Such a mechanism provides a plausible explanation for the high activity observed for Cu@HOF. By contrast, an alternative pathway involving a π-complexation mechanism for alkyne reduction[6] would require a rate-determining protonation step and would not involve radical intermediates.[69,70] In such cases, ethylene formation is insensitive to the presence of TEMPO, and hydrogen evolution and alkyne reduction do not proceed through a shared intermediate. The TEMPO sensitivity observed here, together with the competition between hydrogen evolution and acetylene reduction, therefore rules out a π-

complexation pathway and supports a Cu-hydride-mediated HAT mechanism for acetylene semi-hydrogenation in Cu@HOF. The catalytic cycle is completed by a second protonation step, releasing ethylene and regenerating the Cu(II) species, thereby closing the photocatalytic cycle.

Conclusions

In conclusion, we have reported the first example of a copper-based photocatalyst for the selective semi-hydrogenation of acetylene to ethylene and the first demonstration of a hydrogen-bonded organic framework (HOF) operating as an all-in-one photocatalyst for this industrially relevant transformation. Overall, this work represents an important step toward making the reduction of acetylene to ethylene more selective, energy-efficient, and sustainable by offering a light-driven strategy that uses water as the proton source. Beyond this general advance, the present study establishes two key conceptual contributions: the introduction of copper as an active metal for photocatalytic acetylene purification and the validation of hydrogen-bonded organic frameworks as a viable and powerful platform for light-driven acetylene hydrogenation chemistry.

The use of copper is particularly significant from both a scientific and technological perspective. Copper is earth-abundant, inexpensive, and widely employed in industrial catalysis, yet it has remained essentially unexplored for photocatalytic acetylene semi-hydrogenation. At the same time, the use of a HOF scaffold introduces distinct advantages over more established framework materials such as MOFs and COFs, including mild synthetic accessibility, high modularity, and facile post-synthetic metallation. In Cu@HOF, these features enable the integration of light absorption, charge separation, and catalysis within a single material, eliminating the need for external photosensitizers. Moreover, operation in water, which serves simultaneously as solvent and proton source, represents a major practical advantage over previously reported framework-based photocatalytic systems.

Beyond these conceptual advances, Cu@HOF exhibits striking catalytic performance. Under a pure acetylene feed, the photocatalyst achieves an overall ethylene production of 3.01 mol g^{-1} Cu, corresponding to a 2–100-fold improvement over previously reported framework-based catalysts that work in tandem with a $Ru(bpy)_3^{2+}$, whereas Cu@HOF operates as an all-in-one system.[7,8,10,14,18] Importantly, this high activity is coupled with a ≥99.9% selectivity and is achieved without the use of molecular hydrogen or organic solvents. The Cu@HOF photocatalyst is also highly competent under industrially relevant ethylene purification conditions, namely in the presence of excess ethylene. Under these competitive conditions, near-quantitative conversion of acetylene to ethylene is achieved within 75 min, representing a 3–77-fold improvement over previously reported $Ru(bpy)_3^{2+}$-sensitized framework catalysts.[7,8,10,14,18] The photocatalyst can be readily recovered and reused, retaining catalytic activity over at least four consecutive cycles. An attractive future opportunity would be to merge the acetylene adsorption capacity of HOF materials with the photocatalytic properties reported here. Mechanistic investigations reveal that visible-light excitation of the HOF generates photogenerated electrons that reduce Cu(II) to Cu(I), enabling formation of Cu–H intermediates that mediate acetylene reduction *via* a HAT pathway. Isotope-labelling experiments unambiguously demonstrate that the hydrogen atoms incorporated into the ethylene product originate from water.

Taken together, this work establishes copper-functionalized HOFs as a compelling and versatile platform for sustainable acetylene purification and sets the stage for future developments that exploit the synergy between earth-abundant metal catalysis and hydrogen-bonded frameworks for light-driven chemical transformations.

Author contributions

B. A. and A. F. contributed equally. F. A. and L. Đ. proposed and supervised the project. F. A., L. Đ., B. A. and A. F. designed the experiments. B. A. synthesized the materials. B. A. and A. F. characterized the materials. B. A., A. F. and S. S. performed the photocatalytic experiments. M. B. performed TEM and EPR measurements. B. A. and S. A. designed, performed and analyzed XPS measurements. B. A. and F. A. wrote the manuscript. All authors were involved in manuscript revision and have approved the final version of the manuscript.

Conflicts of interest

There are no conflicts to declare.

Data availability

The data supporting this article have been included as part of the supplementary information (SI). Supplementary information: Fig. S1–S16 and Tables S1 and S2 and further experimental details. See DOI: https://doi.org/10.1039/d6ta00654j.

Acknowledgements

This work was funded with the contribution of the Italian Ministry of University and Research under D.D. n. 1236 of 01/08/2023 – FIS 2 call (ENGCAT, FIS-2023-02956, C53C25000170001, F. A. as Principal Investigator), and by the European Union – NextGenerationEU and the STARS@UNIPD programme. The work carried out in the Đorđević laboratory was supported by the European Union (ERC, PhotoDark, 101077698). Views and opinions expressed are however those of the author(s) only and do not necessarily reflect those of the European Union or the European Research Council. Neither the European Union nor the granting authority can be held responsible for them.

References

1 R. Geyer, J. R. Jambeck and K. L. Law, *Sci. Adv.*, 2017, **3**, e1700782.
2 D. S. Sholl and R. P. Lively, *Nature*, 2016, **532**, 435–437.
3 A. Borodziński and G. C. Bond, *Catal. Rev.*, 2006, **48**, 91–144.

4 F. Studt, F. Abild-Pedersen, T. Bligaard, R. Z. Sørensen, C. H. Christensen and J. K. Nørskov, *Science*, 2008, **320**, 1320–1322.
5 M. Armbrüster, K. Kovnir, M. Friedrich, D. Teschner, G. Wowsnick, M. Hahne, P. Gille, L. Szentmiklósi, M. Feuerbacher, M. Heggen, F. Girgsdies, D. Rosenthal, R. Schlögl and Yu. Grin, *Nat. Mater.*, 2012, **11**, 690–693.
6 F. Arcudi, L. Đorđević, N. Schweitzer, S. I. Stupp and E. A. Weiss, *Nat. Chem.*, 2022, **14**, 1007–1012.
7 A. E. B. S. Stone, L. Đorđević, S. I. Stupp, E. A. Weiss, F. Arcudi and J. T. Hupp, *ACS Energy Lett.*, 2023, **8**, 4684–4693.
8 H. Dai, R. Zhang, Z. Liu, W. Jiang and Y. Zhou, *Chem.–Eur. J.*, 2024, **30**, e202302816.
9 L. Đorđević and F. Arcudi, *Nat. Catal.*, 2025, **8**, 625–626.
10 A. E. B. S. Stone, A. Fortunato, X. Wang, E. Saggioro, R. Q. Snurr, J. T. Hupp, F. Arcudi and L. Đorđević, *Adv. Mater.*, 2025, **37**, 2408658.
11 A. Fortunato, D. Perilli, A. Dron, V. Celorrio, G. Dražić, L. Đorđević, L. Calvillo, C. Di Valentin and F. Arcudi, *Small Methods*, 2025, 2500527.
12 Y. Hu, S. Wang, Z. Jiang, W. Gong, A. Chen, Q. Liu, G. Liu, Z. Shen, J. Low, J. Ma, J. Jiang, C. Gao and Y. Xiong, *ACS Catal.*, 2025, **15**, 1135–1146.
13 T. Huang, P. Du and Y. Lin, *Chin. J. Chem.*, 2025, **43**, 2566–2587.
14 P. Huang, M. Yang, S. Zhang, Z. Li, H. Zhang, S. Wang, Y. Peng, M. Zhang, S. Li, M. Lu and Y. Lan, *Angew. Chem.*, 2025, **137**, e202423091.
15 Z. Wang, F. Xie, J. Liu, X. Jian, Y. Wang, Y. Wang, C. Fan, R. Li and J. Wang, *Small*, 2025, **21**, 2503604.
16 H. Dai, Y. Wang, K. Wang, H. Kang, X. Chen, B. Ding, X. Chen, Y. Du, L. Dong, W. Zhong, N. Sun, P. Liu, C. Yu, J. Ma, F. Song, Y. Hu, S. Tang, Y. Liu, W. Jiang, Y. Su, J. Li and Y. Zhou, *Nat. Catal.*, 2025, **8**, 645–656.
17 X. Lei, C. Lei, X. Wang, W. Chen, Q. Guo, Y. Hu, J. Liu, T. Wang and B. Huang, *Angew. Chem., Int. Ed.*, 2025, **137**, e202511422.
18 Y. Liu, Z. Li, M. Yang, S. Zhang, H. Zhang, Y. Chen, M. Zhang, S. Li, M. Lu and Y. Lan, *Angew. Chem., Int. Ed.*, 2026, e22056.
19 M. Deng, Z. He, Y. Pang, R. Bai, T. Xie, J. Zhang, L. Li and J. Zhang, *Angew. Chem., Int. Ed.*, 2026, e24752.
20 S. Cao, J. Low, J. Yu and M. Jaroniec, *Adv. Mater.*, 2015, **27**, 2150–2176.
21 Y. Chen and D. Jiang, *Acc. Chem. Res.*, 2024, **57**, 3182–3193.
22 L. Zeng, X. Guo, C. He and C. Duan, *ACS Catal.*, 2016, **6**, 7935–7947.
23 B. Wang, R.-B. Lin, Z. Zhang, S. Xiang and B. Chen, *J. Am. Chem. Soc.*, 2020, **142**, 14399–14416.
24 X. Liu, G. Liu, T. Fu, K. Ding, J. Guo, Z. Wang, W. Xia and H. Shangguan, *Adv. Sci.*, 2024, **11**, 2400101.
25 Z. Xiong, S. Xiang, Y. Lv, B. Chen and Z. Zhang, *Adv. Funct. Mater.*, 2024, **34**, 2403635.
26 T. Ren, X. Yu, Y. Huang, Z. Di and C. Li, *Chin. J. Chem.*, 2025, **43**, 165–3170.
27 W.-K. Qin, C.-H. Tung and L.-Z. Wu, *J. Mater. Chem. A*, 2023, **11**, 12521–12538.
28 Y. Gong, D. Zhong and T. Lu, *Angew. Chem., Int. Ed.*, 2025, **64**, e202424452.
29 S. Goswami, K. Ma, J. Duan, K. O. Kirlikovali, J. Bai, J. T. Hupp, P. Li and O. K. Farha, *Langmuir*, 2022, **38**, 1533–1539.
30 C. M. Aitchison, C. M. Kane, D. P. McMahon, P. R. Spackman, A. Pulido, X. Wang, L. Wilbraham, L. Chen, R. Clowes, M. A. Zwijnenburg, R. S. Sprick, M. A. Little, G. M. Day and A. I. Cooper, *J. Mater. Chem. A*, 2020, **8**, 7158–7170.
31 N. Zhang, Q. Yin, S. Guo, K.-K. Chen, T.-F. Liu, P. Wang, Z.-M. Zhang and T.-B. Lu, *Appl. Catal., B*, 2021, **296**, 120337.
32 Q. Zhou, Y. Guo and Y. Zhu, *Nat. Catal.*, 2023, **6**, 574–584.
33 L. Yang, J. Yuan, G. Wang, Q. Cao, C. Zhang, M. Li, J. Shao, Y. Xu, H. Li and J. Lu, *Adv. Funct. Mater.*, 2023, **33**, 2300954.
34 C. Lu, W. Shi, Y. Gong, J. Zhang, Y. Wang, J. Mei, Z. Ge, T. Lu and D. Zhong, *Angew. Chem.*, 2024, **136**, e202405451.
35 S. Wang, W. Guo, C. Li, B. Weng, S. Liu, N. Han, J. Long and H. Zhang, *J. Mater. Chem. A*, 2024, **12**, 12907–12925.
36 J. Mei, S. Lai, Y. Gong, W. Shi, J. Deng, T. Lu and D. Zhong, *Angew. Chem.*, 2025, **137**, e202413413.
37 S. Zhong, H. Shi, C. Xiao, X. Gu, J. Wu, S. Lu, Z. Yuan, Y. Yang, D. Yu and X. Chen, *J. Colloid Interface Sci.*, 2025, **679**, 91–101.
38 R. Gao, R. Shen, C. Huang, K. Huang, G. Liang, P. Zhang and X. Li, *Angew. Chem., Int. Ed.*, 2025, **64**, e202414229.
39 European Commission, *Directorate General for Internal Market, Industry, Entrepreneurship and SMEs, Study on the Critical Raw Materials for the EU 2023: Final Report*, Publications Office, LU, 2023.
40 D. M. Sharma and B. Punji, *Chem.–Asian J.*, 2020, **15**, 690–708.
41 J. Bu, Z. Liu, W. Ma, L. Zhang, T. Wang, H. Zhang, Q. Zhang, X. Feng and J. Zhang, *Nat. Catal.*, 2021, **4**, 557–564.
42 R. Shi, Z. Wang, Y. Zhao, G. I. N. Waterhouse, Z. Li, B. Zhang, Z. Sun, C. Xia, H. Wang and T. Zhang, *Nat. Catal.*, 2021, **4**, 565–574.
43 Z. Chen, C. Cai and T. Wang, *J. Phys. Chem. C*, 2022, **126**, 3037–3042.
44 X. Jiang, L. Tang, L. Dong, X. Sheng, W. Zhang, Z. Liu, J. Shen, H. Jiang and C. Li, *Angew. Chem., Int. Ed.*, 2023, **62**, e202307848.
45 W. Xue, X. Liu, C. Liu, X. Zhang, J. Li, Z. Yang, P. Cui, H.-J. Peng, Q. Jiang, H. Li, P. Xu, T. Zheng, C. Xia and J. Zeng, *Nat. Commun.*, 2023, **14**, 2137.
46 E. Zhao, W. Zhang, L. Dong, R. Zbořil and Z. Chen, *ACS Catal.*, 2023, **13**, 7557–7567.
47 F. Studt, F. Abild-Pedersen, T. Bligaard, R. Z. Sørensen, C. H. Christensen and J. K. Nørskov, *Science*, 2008, **320**, 1320–1322.
48 F. Pape, N. O. Thiel and J. F. Teichert, *Chem.–Eur. J.*, 2015, **21**, 15934–15938.
49 K. Semba, R. Kameyama and Y. Nakao, *Synlett*, 2015, **26**, 318–322.
50 T. Wakamatsu, K. Nagao, H. Ohmiya and M. Sawamura, *Organometallics*, 2016, **35**, 1354–1357.

51 *Homogeneous Hydrogenation with Non-Precious Catalysts*, ed. J. F. Teichert, 2019.
52 S. E. Sloane, A. Reyes, Z. P. Vang, L. Li, K. T. Behlow and J. R. Clark, *Org. Lett.*, 2020, **22**, 9139–9144.
53 Z. Wang, L. Shang, H. Yang, Y. Zhao, G. I. N. Waterhouse, D. Li, R. Shi and T. Zhang, *Adv. Mater.*, 2023, **35**, 2303818.
54 Q. Gao, Z. Yan, W. Zhang, H. S. Pillai, B. Yao, W. Zang, Y. Liu, X. Han, B. Min, H. Zhou, L. Ma, B. Anaclet, S. Zhang, H. Xin, Q. He and H. Zhu, *J. Am. Chem. Soc.*, 2023, **145**, 19961–19968.
55 X. Jiang, L. Tang, L. Dong, X. Sheng, W. Zhang, Z. Liu, J. Shen, H. Jiang and C. Li, *Angew. Chem., Int. Ed.*, 2023, **62**, e202307848.
56 J. C. De Almeida, Y. Wang, T. A. Rodrigues, P. H. H. Nunes, V. R. De Mendonça, P. H. E. Falsetti, L. V. Savazi, T. He, A. V. Bardakova, A. V. Rudakova, J. Tian, A. V. Emeline, O. F. Lopes, A. O. T. Patrocínio, J. H. Pan, C. Ribeiro and D. W. Bahnemann, *Adv. Funct. Mater.*, 2025, 2502901.
57 W. Zhai, Y. Ma, D. Chen, J. C. Ho, Z. Dai and Y. Qu, *InfoMat*, 2022, **4**, e12357.
58 N. Liu, J. Jiang, Z. Chen, B. Wu, S. Zhang, Y. Zhang, P. Cheng and W. Shi, *Angew. Chem., Int. Ed.*, 2023, **62**, e202312306.
59 X. Peng, M. Zhang, H. Qin, J. Han, Y. Xu, W. Li, X. Zhang, W. Zhang, U. Apfel and R. Cao, *Angew. Chem., Int. Ed.*, 2024, **63**, e202401074.
60 K. S. Rawat, S. Borgmans, T. Braeckevelt, C. V. Stevens, P. Van Der Voort and V. Van Speybroeck, *ACS Appl. Nano Mater.*, 2022, **5**, 14377–14387.
61 K. Ma, P. Li, J. H. Xin, Y. Chen, Z. Chen, S. Goswami, X. Liu, S. Kato, H. Chen, X. Zhang, J. Bai, M. C. Wasson, R. R. Maldonado, R. Q. Snurr and O. K. Farha, *Cell Rep. Phys. Sci.*, 2020, **1**, 100024.
62 J. Conradie and E. Erasmus, *J. Electron Spectrosc. Relat. Phenom.*, 2022, **259**, 147241.
63 Q. Yin, P. Zhao, R. Sa, G. Chen, J. Lü, T. Liu and R. Cao, *Angew. Chem.*, 2018, **130**, 7817–7822.
64 G. Chen, S. Huang, Y. Shen, X. Kou, X. Ma, S. Huang, Q. Tong, K. Ma, W. Chen, P. Wang, J. Shen, F. Zhu and G. Ouyang, *Chem*, 2021, **7**, 2722–2742.
65 P. Zhang, M. Wang, Y. Yang, T. Yao and L. Sun, *Angew. Chem., Int. Ed.*, 2014, **53**, 13803–13807.
66 A. Z. Haddad, S. P. Cronin, M. S. Mashuta, R. M. Buchanan and C. A. Grapperhaus, *Inorg. Chem.*, 2017, **56**, 11254–11265.
67 J. Wang, C. Li, Q. Zhou, W. Wang, Y. Hou, B. Zhang and X. Wang, *Dalton Trans.*, 2016, **45**, 5439–5443.
68 S. Fukuzumi, Y.-M. Lee and W. Nam, *Coord. Chem. Rev.*, 2018, **355**, 54–73.
69 S. Gnaim, A. Bauer, H.-J. Zhang, L. Chen, C. Gannett, C. A. Malapit, D. E. Hill, D. Vogt, T. Tang, R. A. Daley, W. Hao, R. Zeng, M. Quertenmont, W. D. Beck, E. Kandahari, J. C. Vantourout, P.-G. Echeverria, H. D. Abruna, D. G. Blackmond, S. D. Minteer, S. E. Reisman, M. S. Sigman and P. S. Baran, *Nature*, 2022, **605**, 687–695.
70 G. Durin, M.-Y. Lee, M. A. Pogany, T. Weyhermüller, N. Kaeffer and W. Leitner, *J. Am. Chem. Soc.*, 2023, **145**, 17103–17111.

